Carbohydrate Polymers 86 (2011) 1327–1335

Contents lists available at ScienceDirect

Carbohydrate Polymers

journal homepage: www.elsevier.com/locate/carbpol

Optimization, dynamics, and enhanced production of a free radical scavenging extracellular polysaccharide (EPS) from hydrodynamic sediment attached *Bacillus megaterium* RB-05

Sougata Roy Chowdhury[a], Ratan Kumar Basak[a], Ramkrishna Sen[b,*], Basudam Adhikari[a]

[a] *Materials Science Centre, Indian Institute of Technology Kharagpur, WB 721302, India*
[b] *Department of Biotechnology, Indian Institute of Technology Kharagpur, WB 721302, India*

ARTICLE INFO

Article history:
Received 31 January 2011
Received in revised form 14 June 2011
Accepted 15 June 2011
Available online 23 June 2011

Keywords:
Bacillus megaterium RB-05
Extracellular polysaccharide
Optimization
Dynamics
Free radical scavenger

ABSTRACT

Extracellular polysaccharide production of *Bacillus megaterium* RB-05, a river sediment isolate, was optimized in glucose mineral salts medium by response surface methodology. Experimental maximum production (0.895 g l^{-1}) was very close to the theoretical maximum value of 0.904 g l^{-1} after 25 h incubation at 33.3 °C and pH 7.62. The maximum specific growth rate and specific EPS production rate were calculated to be 0.65 h^{-1} and 0.215 g g^{-1} cell respectively. The growth yield coefficient and product yield coefficients were evaluated to be 0.13 g of biomass g^{-1} glucose, 0.065 g of EPS g^{-1} glucose, and 0.484 g of EPS g^{-1} biomass. Yields were enhanced up to 1.2 g l^{-1} with L-aspergine and D-biotin supplementation. EPS showed evidence of free radical scavenging in *in vitro* studies.

1. Introduction

Multifunctionalized polysaccharide molecules of plant, bacterial and fungal origin have been extensively researched in last the few decades. Until now macromolecules of plant origin have captured the commercial market for their ease of availability and cost-effective purification process. But renewability, stable cost, constant and reproducible physico-chemical properties of the microbial polysaccharides have provided them an edge over the macromolecules of plant origin, although only few of them have been commercialized so far (Sutherland, 2001; Vanhaverbeke, Heyraud, & Mazeau, 2003). Recently these novel bioactive chemical compounds have been introduced in different medicinal and therapeutic applications. These molecules are successfully used for antioxidant, anti-tumor, anti-inflammatory, and anti-viral activities. Extracellular polysaccharides (EPS) are also found to induce interferon and cytokine activity, inhibit platelet aggregation, stimulate colony stimulating factors, and modulate immune system (Calazans, Lopes, Lima, & De Franc, 1997)

Free radicals, especially those belonging to the family of reactive oxygen species (ROS), are increasingly recognized as a cause of aging and in the pathogenesis of different human diseases including cancer. Oxidative damage to the cellular molecules caused by the chain reactions of the free radicals can be countered with antioxidants or free radical scavengers (Chen, Zhang, & Xie, 2005; Kishk & Al-Sayed, 2007). Different antioxidants of synthetic origin are commercially available, although many of them were found to have some side effects in recent studies. Hence, natural antioxidants with lower side-effects and better bio-acceptability will become increasingly important. It has been shown that many polysaccharides of plant and microbial origin displayed radical scavenging or antioxidant property because of their abundance of functional groups (Liu et al., 2009).

It is important to design the optimal production medium, process parameters, and set of operating conditions to achieve a high yield process system for microbial EPS production. Usually the production parameters are optimized considering only single factor at a time without taking account of interactions between parameters (Francis et al., 2003). Further, this method is time consuming and requires a large number of experiments to determine the optimum levels in the production medium. These limitations of the single factor optimization method can be overcome by developing a non-linear multivariate process model. Response surface methodology (RSM) is a well-known method applied in the optimization of medium constituents and other critical variables responsible for the production of biomolecules (Montgomery, 1997). Statistical experimental designs can be employed at various phases of optimization process, such as for screening experiments and for finding optimum

* Corresponding author. Tel.: +91 3222 283752; fax: +91 3222 278707.
E-mail address: rksen@yahoo.com (R. Sen).

0144-8617/$ – see front matter © 2011 Elsevier Ltd. All rights reserved.
doi:10.1016/j.carbpol.2011.06.050

conditions for a desired response. This method has been successfully applied in the optimization of media composition (Roseiro, 1992; Souza, Roberto, & Milagres, 1999) and fermentation processes (Jiao, Chen, Zhou, Zhang, & Chen, 2008; Kalil, Maugeri, & Rodrigues, 2000).

This present work was carried out to optimize the production parameters and to study the production dynamics of the EPS, isolated from a riverine sediment-attached *Bacillus megaterium* RB-05 [GenBank accession number HM371417]. Effect of different nutrient resources on microbial growth and EPS yield was thoroughly studied. The EPS was also partially characterized and *in vitro* free radical scavenging potential of the material was analyzed for possible therapeutic applications.

2. Materials and methods

2.1. Isolation and identification of bacteria

The strain was isolated from the sediment of river Rupnarayan (pH 7.2), West Bengal, India. The strain was selected on the basis of EPS production in nitrogen-free glucose mineral salts media (GMSM). The composition of GMSM was glucose (2%), NH_4NO_3 (0.3%); K_2HPO_4 (0.22%); KH_2PO_4 (0.014%); NaCl (0.001%); $MgSO_4$ (0.06%); $CaCl_2$ (0.004%); $FeSO_4$ (0.002%) and 0.05% trace elements solution (2.32 g l^{-1} of $ZnSO_4{\cdot}7H_2O$; 1.78 g l^{-1} of $MnSO_4{\cdot}4H_2O$; 0.56 g l^{-1} of H_3BO_3; 1.0 g l^{-1} of $CuSO_4{\cdot}5H_2O$; 0.39 g l^{-1} of $Na_2MoO_4{\cdot}2H_2O$; 0.42 g l^{-1} of $CoCl_2{\cdot}6H_2O$; 1.0 g l^{-1} of EDTA; 0.004 g l^{-1} of $NiCl_2{\cdot}6H_2O$ and 0.66 g $l^{-1}$of KI). The selected strain was identified by 16S rDNA sequencing. Extraction of total genomic DNA from the isolate was done following Sambrook, Fritsch, and Maniatis (1989). Universal primer 27 F [5′-AGAGTTTGATCMTGGCTCAG-3′] and 1518R [5′-AAGGAGGTGWTCCARCC-3′] was used for amplification of 16S rDNA gene by PCR. A PCR mixture of 50 ng of extracted genomic DNA, 1 μl (100 ng each) of the primers, and 50 μl reaction buffer containing 10 mM dNTP, 1.5 mM $MgCl_2$ and 3 units Taq polymerase (Bangalore Genei, India) was prepared. PCR was performed using a thermocycler (Bangalore Genei, India). Conditions set for polymerase chain reactions were an initial denaturation for 5 min at 94 °C followed by 30 cycles for denaturation at 94 °C for 30 s, annealing at 55 °C for 30 s, extension at 72 °C for 30 s a final extension step at 72 °C for 7 min. PCR products were analyzed by 1.0% agarose gel electrophoresis, stained with ethidium bromide and visualized under UV-transilluminator. The PCR amplified DNA was eluted from gel and purified by QIA quick gel extraction kit (QIAGEN). Sequencing was done using Bigdye terminator kit (ABI) and same primers (used for PCR) in an automated DNA sequencer (ABI model 3100, Hitachi). The sequence was compared with those available in the GenBank databases using BLAST (Pearson & Lipman, 1988) and phylogenetic analysis was done using MEGA version 3.1 program by NJ (Neighborhood Joining)/MP (Maximum Parsimony) method (Kumar, Tamura, & Nei, 2004).

2.2. Production optimization with different parameters

In the present work, RSM based on Box Behnken Design (BBD) was used to investigate the significance of the combined effects of incubation time (h), incubation temperature (°C), and media pH on EPS production. Initial ranges of these independent variables were chosen according to information from the literature, and initial experiments. All the experiments were conducted in triplicate. A three-level, three-factor factorial BBD with center points leading to 15 runs (12 organized in a fractional factorial design and 3 involving replications of the central points) was developed by MINITAB 15 software for the optimization. The series of experiments designed and conducted are shown in Table 1 in coded and uncoded terms. In coded terms the lowest, central and the highest levels of three variables are −1, 0, and +1 respectively. The experimental data were analyzed by the Response Surface Regression (RSREG) procedure to fit the following second-order polynomial equation (Eq. (1)) (Zheng et al., 2008):

$$Y = \beta_{k0} + \sum_{i=1}^{3} \beta_{ki} x_i^2 + \sum_{i=1}^{3} \beta_{kii} x_i^2 \quad (1)$$

where Y is response (g l^{-1} EPS production); β_{k0}, β_{ki}, β_{kii} are the constant coefficients and x_i, is the coded independent variable, which influences the response variable Y.

2.3. Effects of different carbon, nitrogen and vitamin sources

Different carbon sources (glucose, galactose, mannose, sucrose, xylose, arabinose, fructose, lactose, and glycerol) were introduced to the mineral salts medium to determine the effect of carbon dose on EPS production. Individual effect of different nitrogen sources (glutamic acid, L-aspergine, casamino acid, sodium nitrate, potassium nitrate, ammonium chloride, L-tryptophan and glycine) and vitamin sources (thiamine, riboflavin, cyanocobalamine, D-biotin and pyridoxal phosphate) on microbial growth and EPS production were also examined. Growth of the organism was determined in terms of optical density measured at 600 nm.

2.4. Growth and production dynamics

A knowledge for the kinetics is always crucial for scaling up fermentation reactions. In certain cases, microbial processes follow some classical kinetic models. One of these was proposed by Monod (1949) related to the substrate-limited biomass growth and product formation during fermentation. Kono and Asai (1969) also studied product formation behavior and established a relationship with biomass concentration. Luedeking and Piret (1959) proposed another model to correlate product formation and growth. According to this model, the product formation rate depends on both the instantaneous biomass concentration and the growth rate in a linear manner.

Microbial growth kinetics can be described by an empirical model (Eq. (2)) originally proposed by Monod (1949). The Monod model introduced the concept of a growth limiting substrate.

$$\mu = \mu_{\max} \frac{S}{K_s + S} \quad (2)$$

where μ = specific growth rate, $\mu_{\max}$ = maximum specific growth rate, S = substrate concentration, K_s = substrate saturation constant (i.e. substrate concentration at half $\mu_{\max}$). In Monod's model, the growth rate is related to the concentration of a single growth-limiting substrate through the parameters $\mu_{\max}$ and K_s. In addition to this, Monod model is also related to different yield coefficients (growth yield coefficient, $Y_{X/S}$ and product yield coefficient, $Y_{P/S}$).

The kinetics of product formation was analyzed based on the Luedeking–Piret's equation (Eq. (3)) (1959). According to this model, the product formation rate depends on both the instantaneous biomass concentration (N) and the growth rate in a linear manner.

$$\frac{dP}{dt} = \alpha \frac{dN}{dt} + \beta N \quad (3)$$

where α and β are the product formation constants and may differ under different fermentation conditions. It is easier to verify this

Table 1
Experimental design (conditions and responses) for EPS production by *B. megaterium* RB-05 in GMSM, in terms of coded factor.

Run order	*A*	*B*	*C*	EPS yield ($g l^{-1}$)	
				Experimental value	Fit value
1	−1(20)	−1(30)	0(7.5)	0.476 ± 0.028	0.488
2	0(24)	0(34)	0(7.5)	0.839 ± 0.047	0.862
3	0(24)	−1(30)	+1(8.0)	0.689 ± 0.039	0.702
4	0(24)	+1(38)	+1(8.0)	0.571 ± 0.034	0.620
5	−1(20)	+1(38)	0(7.5)	0.471 ± 0.024	0.447
6	0(24)	−1(30)	−1(7.0)	0.616 ± 0.041	0.566
7	+1(28)	0(34)	−1(7.0)	0.519 ± 0.029	0.544
8	−1(20)	0(34)	−1(7.0)	0.378 ± 0.019	0.414
9	+1(28)	+1(38)	0(7.5)	0.592 ± 0.033	0.579
10	+1(28)	0(34)	+1(8.0)	0.746 ± 0.042	0.709
11	0(24)	0(34)	0(7.5)	0.884 ± 0.049	0.862
12	0(24)	0(34)	0(7.5)	0.864 ± 0.051	0.862
13	−1(20)	0(34)	+1(8.0)	0.532 ± 0.029	0.506
14	+1(28)	−1(30)	0(7.5)	0.665 ± 0.037	0.688
15	0(24)	+1(38)	−1(7.0)	0.513 ± 0.027	0.499

assumed relationship and to evaluate the constants if the equation (Eq. (3)) be modified dividing by N to give

$$\frac{1}{N}\frac{dP}{dt} = \frac{\alpha}{N}\frac{dN}{dt} + \beta \quad (4)$$

Since, by definition, $k = (1/N)(dN/dt)$, the equation (Eq. (5)) finally simplifies to

$$\frac{1}{N}\frac{dP}{dt} = \alpha k + \beta \quad (5)$$

The constants α and β were determined from the plots, where α is equal to the slope of the straight line and β is equal to the $(1/N)(dP/dt)$ intercept. The relationship between dP/dt (rate of product accumulation) and dx/dt (rate of biomass formation) as a function of biomass concentration (x) was established following the model proposed by Kono and Asai (1969).

2.5. Isolation and chemical analysis of exopolysaccharides

The crude EPS was isolated from RB-05 culture following the method described by Sharon and Jeanloz (1960) with slight modifications. The 24 h culture was centrifuged at 10,000 rpm for 20 min at 4 °C. The supernatant was filtered through 0.22 μm membrane filter (Millipore Co., Cork, Ireland). Protein precipitation was done by adding two volumes of 10% trichloroacetic acid (TCA) to the filtrate, and kept overnight at 4 °C in static condition and then recentrifuged at 15,000 rpm for 20 min. Polysaccharides were precipitated by adding four volumes of prechilled 95% ethanol to the supernatant, further kept for 24 h at 4 °C and centrifuged at 15,000 rpm for 20 min at 4 °C. The pellet was lyophilized to get the dry powder of the EPS. The powder was dissolved in 5 ml distilled water and dialyzed using 14 kDa cut off dialysis membrane (Himedia, India) in order to separate molecules less than 14 kDa. The dialyzed EPS was relyophilized and analyzed for carbohydrate and protein contents. Carbohydrate content was determined spectrophotometrically at 490 nm following phenol-sulfuric acid method (Dubois, Gilles, Hamilton, Rebers, & Smith, 1956) and protein content was also determined spectrophotometrically using 750 Lambda Double Beam UV–Vis Spectrophotometer (Perkin Elmer,) at 595 nm (Lowry, Rosebrough, Farr, & Randall, 1951). Elemental composition of the material was analyzed using CHN elemental analyzer. FT-IR spectrum for the polysaccharide sample was acquired with Thermo Nicolet Nexus 870 Spectrophotometer in the absorbance mode. Compressed pellets were prepared by mixing 2 mg of pre-conditioned EPS with 100 mg of KBr. Spectrum was corrected for KBr background using the OMNIC software and recorded in the range 4000–400 cm^{-1} using 32 scans. RIGAKU X-ray diffractometer (ULTIMA III) was used in XRD analysis of the EPS material. The samples were examined in powder form maintaining the operating 2θ range between 10° and 50° at a scanning speed of 2°/min using Cu Kα radiation.

2.6. Morphology study

Surface morphology of the polymer samples (from the culture broth) was studied under scanning electron microscope (SEM) and field emission scanning electron microscope (FeSEM). For both of these microscopic analyses sample was washed three times with aqueous 1% osmium tetroxide solution for 2 h at 4 °C and dehydrated in ethanol series (50, 80, 90 and saturated) followed by critical point drying. Gold sputtering on the samples was done using a SCD 050 coater (Bal-Tec, Wallruf, Germany). All the samples were examined under VEGA TESCAN SEM at 10 kV and SUPRA 40, ZEISS SMT AG (Germany) FeSEM at 5 kV. For transmission electron microscope (TEM) specimens were fixed with 2.5% glutaraldehyde in PBS buffer containing 0.15% ruthenium red for 2 h at room temperature. Fixed material was then washed three times with aqueous 1% osmium tetroxide for 2 h at 4 °C and rewashed five times with buffer following dehydration in ethanol series (50, 80, 90 and saturated). Ruthenium red was maintained at 0.05% in all solutions up to 80% ethanol. Uranyl acetate stained material cast on copper grid, after critical point drying, was examined under ZEISS TEM at an accelerated voltage of 60 kV.

2.7. Determination of free radical scavenging activities

Measurements of superoxide radical scavenging activities of the samples and standard quercetin were done based on the reduction of nitro blue tetrazolium (NBT). Superoxide radicals were generated by a non-enzymatic system of phenazine methosulfate/nicotinamide adenine dinucleotide (PMS/NADH). These radicals reduced NBT to a purple coloured formazan, which was measured spectrophotometrically at 562 nm. In hydroxyl radical scavenging assay, radicals were generated by the Fenton reaction using a Fe^{3+}–ascorbate–EDTA–H_2O_2 system. The assay quantifies the 2-deoxyribose degradation product, by its condensation with TBA. Ascorbic acid was used as standard hydroxyl radical scavenger. For the assay of DPPH radical scavenging aliquots of the EPS (0.2 ml, 0–1000 $\mu g\,ml^{-1}$) and positive control (ascorbic acid) were individually mixed with the 100 mM Tris–HCl buffer (0.8 ml, pH 7.4) and then added to 1 ml of 500 μM DPPH in ethanol. The mixture was shaken vigorously and left in the dark at room temperature for 20 min. The absorbance of the resulting solution was measured spectrophotometrically at 517 nm. All the measurements were repeated six times.

3. Results and discussion

3.1. Response surface method (RSM)

The experimental data were first analyzed in order to determine the second-order equations including terms of interaction between the experimental variables. The equation (Eq. (6)) given below is based on the statistical analysis of the experimental data shown in Table 1. The mathematical expression of relationship of EPS production by *B. megaterium* RB-05 with variables *A*, *B*, and *C* (incubation time, temperature, and pH respectively) are given below in terms of coded factors.

$$Y = -46.5 + 0.535A + 0.578B + 8.142C - 0.011AA - 0.008BB - 0.544CC - 0.001AB + 0.009AC - 0.001BC \quad (6)$$

Based on the experimental response, the EPS production was increased from 0.378 g l^{-1} to 0.884 g l^{-1}. Runs 8 and 11 had the minimum and maximum production respectively. The quadratic regression model for EPS yield is given in Table 2a. ANOVA of the regression model (Table 2b) for EPS production demonstrated that the model was significant due to *F*-value (15.38) and R^2 value (0.96). Only less than 4% of the total variations were not explained by the model and the *F* value indicated that EPS production in GMSM had a good model fit. The *P* values were used as a tool to check the significance of each coefficient and the interaction strength between each independent variable. The smaller the *P* values, the bigger are the significance of the corresponding coefficient (Cui et al., 2006).

The combined effect of incubation temperature and pH is shown in Fig. 1a. EPS production was increased with the increasing temperature but after specific temperature (33.3 °C), this trend reversed as EPS yield started to fall. Significant increase in EPS production was observed up to pH 7.62 and after that increasing the pH reduced the EPS yield. Incubation temperature with pH had significant impact on EPS production in GMSM by *B. megaterium* RB-05.

Table 2a
Results of regression analysis of correlating optimized parameters by second-order polynomial model.

Model term	Regression coefficient	Std. deviation	*t*-Statistics	*P*-Value
Intercept	−46.500	7.359	−6.31	0.001
A	0.535	0.128	4.17	0.009
B	0.578	0.144	3.99	0.010
C	8.142	1.588	5.12	0.004
AA	−0.011	0.001	−7.26	0.001
BB	−0.008	0.001	−5.13	0.004
CC	−0.544	0.100	−5.42	0.003
AB	−0.001	0.001	−0.70	0.512
AC	0.009	0.012	0.75	0.483
BC	−0.001	0.012	−0.15	0.883

Table 2b
ANOVA analysis of RSM model for process fitness.

Source	DF[a]	Seq SS[b]	Adj SS[b]	Adj MS[c]	*F*	*P*
Regression	9	0.322	0.322	0.035	15.38	0.004
Linear	3	0.099	0.103	0.034	14.81	0.006
Square	3	0.220	0.220	0.073	31.55	0.001
Interaction	3	0.002	0.002	0.000	0.36	0.782
Residual error	5	0.011	0.011	0.002		
Lack-of-fit	3	0.010	0.010	0.003	6.97	0.128
Pure error	2		0.001	0.001	0.0005	
Total	14	0.333				
R^2 = 96.51 R^2 (adj) = 90.24%						

[a] Degree of freedom.
[b] Sum of square.
[c] Mean square.

The joint interaction of incubation temperature and time on EPS yield is revealed in Fig. 1b. The maximum EPS (0.884 g l^{-1}) was produced after 25 h incubation at 33.3 °C. In Fig. 1c it was observed that increasing incubation time with the pH accelerated EPS yield and at specific pH (7.62) and incubation time (25 h) EPS production was found maximum (0.884 g l^{-1}). But with further increase in pH with incubation time EPS production slowly started to decrease.

The optimal conditions for EPS production by *B. megaterium* RB-05 in GMSM were estimated by Minitab 15 software. Taking all parameters into consideration, the optimum operating parameters were pH: 7.62, incubation time: 25 h and incubation temperature: 33.3 °C. Under these conditions, the maximum EPS production was about 0.904 g l^{-1}. To confirm the predicted response, experiments were conducted in triplicates. The maximum EPS production was found to be 0.895 g l^{-1}. This was very close to the predicted response. Thus optimization of EPS production by *B. megaterium* RB-05 in GMSM was successfully developed by RSM.

3.2. Production fitness with conventional kinetic models

The most active part of the cell growth curve is the exponential (log) phase, which is used for the determination of different kinetic parameters. The log phase is a period of balanced growth, in which all components of a cell grow at the same rate (Divyashree, Rastogi, & Shamala, 2009). The growth kinetics of *B. megaterium* RB-05 in GMSM under the conditions as mentioned in materials and methods was characterized in terms of the kinetic constants, namely, maximum specific growth rate (μ_{max}) and Monod's constant (K_s). The double reciprocal Lineweaver–Burk plot of the specific growth rates versus corresponding residual substrate concentrations (Fig. 2a) showed that the culture of *B. megaterium* RB-05 had a μ_{max} of 0.65 ± 0.01 h^{-1} and K_S of 31.6 ± 1.4 g l^{-1}. These results demonstrate that this concerned strain grows fast in GMSM with a low affinity for the growth limiting substrate, glucose, as indicated by a high value of K_S. Although the classical Monod equation does not consider the fact that cells may need substrate or may consume their own synthesized products even when they do not grow (Wang et al., 2006).

To define efficient strategies for bioprocesses, it is important to elucidate the degree of interdependence between biomass growth and product formation. For this purpose, the experimental data were analyzed according to the Kono–Asai (1969) classification and Luedeking–Piret's model (1959).

Kono–Asai's (1969) approach analyzes product formation rate (dp/dt) and growth rate (dx/dt) to describe the association between product formation and growth. The values of the differentials dp/dt and dx/dt represented in Fig. 2b were obtained by derivation of the third-order polynomial fitted to the experimental data. This figure exhibits the profile for cell growth rate (dx/dt) and product formation rate (dp/dt) as functions of biomass concentration. Both curves confirm that polysaccharide synthesis by *B. megaterium* RB-05 is growth associated. Maximum product yield was observed during mid and late log phase, whereas, in stationary phase EPS yield almost got seized.

Applying the Luedeking–Piret's model (1959) specific EPS production rates (r_p) and specific growth rates (μ) were correlated by a linear regression (Fig. 2c) and the values for the stoichiometric coefficients α and β were calculated to be 0.215 g g^{-1} cell and 0.0275 g g^{-1} cell h^{-1}, respectively. The correlation coefficient value (r^2 = 0.9249) of this linear model well describes the relationship between product formation rate and cell growth with a high level of confidence. Furthermore, it can be stated that product formation is associated with bacterial growth, since the value estimated for the stoichiometric coefficient α was found higher than the value of the maintenance coefficient β.

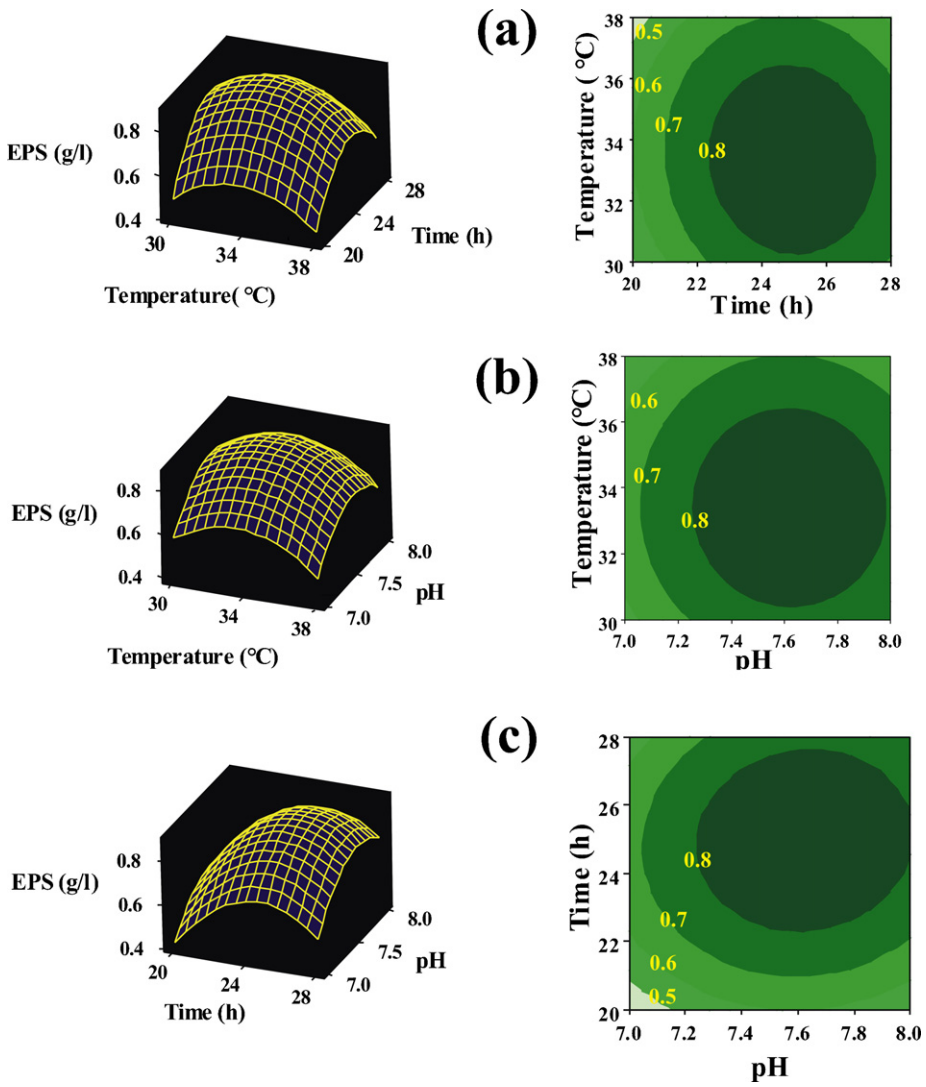

Fig. 1. Response surface plots showing effects of multivariate parameters for the optimization of EPS production in GMSM. Effects of temperature (°C) and pH (a); temperature (°C) and time (h) (b); time (h) and pH (c).

The specific rates, both for growth and of EPS production, were in a sense of measures of the metabolic activity of the individual cells. It is to be expected that if the lag phases could be ignored, the specific rates were found high (Fig. 2d) in the initial log phase of the fermentation, and has declined steadily (Fig. 2d) as the fermentation proceeds due to the disappearance of media nutrients (1959).

The growth yield coefficient ($Y_{X/S}$) was evaluated to be 0.13 ± 0.01 g of biomass g^{-1} glucose. The product yield coefficients, $Y_{P/S}$ and $Y_{P/X}$, were 0.065 ± 0.003 g of EPS g^{-1} glucose and 0.484 ± 0.002 g of EPS g^{-1} biomass, respectively. The experiments were carried out five times and the values were expressed in means ± standard deviations ($n = 5$).

3.3. Effects of different nutrient resources and enhanced production

Glucose was found to be the most suitable for EPS production amongst all the carbon sources experimented (Table 3a). Effective concentration of glucose for maximum yield was in the range of 2–3% (w/v) and that remained almost unchanged up to 4%. Xylose, sucrose and galactose also stimulated the microbial growth and EPS production, but in higher concentrations (3–10%) these sugars retarded the growth rate and causes low product yield (data not shown). Similar observations were also studied with *Fomes fomentarius* (Chen, Zhao, Chen, & Li, 2008) and *Antrodia cinnamomea* (Lin & Chen, 2007). On the other hand, sucrose, as carbon source, was most favorable high EPS production by *Bacillus polymyxa* KCTC 8648P (Lee et al., 1997) and *Bacillus licheniformis* 8-37-0-1(Liu et al., 2009). Different carbon sources may have different catabolic reactions to play during secondary cellular metabolism (Lin & Chen, 2007). Along with carbon, nitrogen as resource also plays an influencing part on EPS production and microbial growth (Panda, Jain, Sharma, & Mallick, 2006). Several nitrogen sources were employed separately in GMSM to monitor the effect on EPS production. L-Aspergine and casamino acid were enacted as good accelerators for growth of bacterial biomass and polysaccharide production (Table 3b). EPS yields were found to be 0.925 ± 0.051 g l^{-1} and 0.918 ± 0.055 g l^{-1} respectively, after addition of 0.5% (w/v) L-aspergine and casamino acid to glucose (2% w/v) mineral salt medium. Supplementation of organic nitrogen was found quite encouraging for microbial growth and EPS yield than inorganic nitrogen salts. Availability of essential amino acids in organic nitrogen constituents

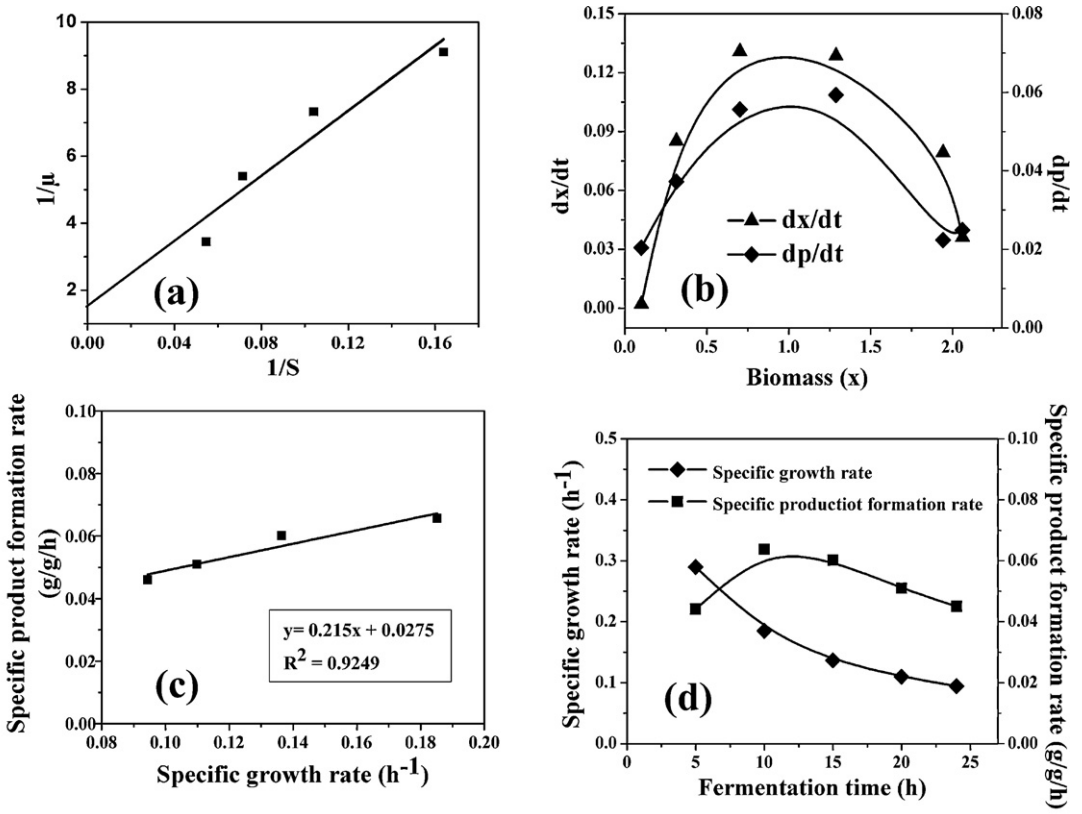

Fig. 2. Kinetics of EPS production by *B. megaterium* RB-05 in GMSM. Double reciprocal plot of specific growth rates versus residual substrate concentrations for the determination of μ_{max} and K_S (a); association between growth and product formation according to Kono–Asai classification (b); linear regression plot of Luedeking–Piret's model specific product formation rates (r_p) and growth rates (μ) (c); specific rate of bacterial growth and of EPS production versus time (d).

make them more favorable as a resource (Shih, Pan, & Hsieh, 2006).

Biomass showed most effective response to low concentration vitamin supplementation. D-Biotin (200 μg l^{-1}) and thiamine (10 μg l^{-1}) accompanied higher EPS yields, 0.968 ± 0.045 g l^{-1} and 0.945 ± 0.045 g l^{-1} respectively, amongst all the vitamins experimented (Table 3c). Vitamins perform a typical catalytic function on cellular metabolism as coenzyme or constituents of coenzyme (Garraway & Evans, 1984). Under the conditions applied in this study, maximum level of EPS (1.12 ± 0.062 g l^{-1}) was obtained after subsequent supplementation of L-aspergine (0.5% w/v), D-biotin (200 μg l^{-1}) in GMSM (Table 3d). Therefore, EPS production and biomass yield of *B. megaterium* RB-05 largely depend upon the media compositions.

3.4. Extracellular biosynthesis, isolation and estimation of EPS

As mentioned above, the EPS produced by *B. megaterium* RB-05 was isolated by alcohol precipitation followed by dialysis and lyophilization. Precipitation by ethanol (95%) removes only the polymers (EPS and proteins) and not the monomers present in the fermentation medium (Kodali, Das, & Sen, 2009). After 25 h, the concentration of EPS was estimated to be 0.895 ± 0.028 g l^{-1} using glucose as standard and that of total protein was estimated to be 0.083 ± 0.024 g l^{-1} using bovine serum albumin (BSA) as standard. The amount of contaminating proteins can further be reduced by repeated precipitation using TCA (García-Garibay & Marshall, 1991). The white coloured lyophilized product was found to be hygroscopic and due care was taken to prevent it from get-

Table 3a
Effect of different carbon sources on growth and EPS production of the *B. megaterium* RB-05.[a]

Carbon sources	Growth (O.D. at 600 nm)	EPS (g l^{-1})
Glucose	1.56 ± 0.09	0.895 ± 0.055
Galactose	1.11 ± 0.09	0.618 ± 0.052
Mannose	0.92 ± 0.08	0.476 ± 0.039
Sucrose	1.31 ± 0.09	0.727 ± 0.068
Xylose	1.19 ± 0.08	0.678 ± 0.051
Arabinose	0.76 ± 0.05	0.359 ± 0.041
Fructose	0.94 ± 0.07	0.471 ± 0.046
Lactose	0.88 ± 0.06	0.411 ± 0.038
Glycerol	0.41 ± 0.06	0.119 ± 0.029

[a] Bacteria were grown in mineral salt media at 33.3 °C for 25 h, pH 7.6 supplemented with different carbon sources (2% w/v). Data are the mean of triplicates ± S.D.

Table 3b
Effect of different nitrogen sources on growth and EPS production of the *B. megaterium* RB-05.[a]

Nitrogen sources	Growth (O.D. at 600 nm)	EPS (g l^{-1})
Control	1.56 ± 0.09	0.895 ± 0.055
Glutamic acid	1.38 ± 0.11	0.823 ± 0.042
L-Aspergine	1.45 ± 0.19	0.925 ± 0.051
Sodium nitrate	0.85 ± 0.10	0.461 ± 0.072
Potassium nitrate	0.77 ± 0.17	0.398 ± 0.067
Ammonium chloride	0.69 ± 0.13	0.311 ± 0.082
L-Tryptophan	1.25 ± 0.21	0.779 ± 0.071
Casamino acid	1.42 ± 0.18	0.918 ± 0.055
Glycine	1.14 ± 0.23	0.720 ± 0.069

[a] Bacteria were grown in GMSM at 33.3 °C for 25 h, pH 7.6 with addition of 0.5 g l^{-1} of nitrogen sources separately except in control. Data are the mean of triplicates ± S.D.

Table 3c
Effect of different vitamin sources on growth and EPS production of the *B. megaterium* RB-05.[a]

Vitamin sources	Growth (O.D. at 600 nm)	EPS ($g\,l^{-1}$)
Control	1.56 ± 0.09	0.895 ± 0.055
Thiamine (10 $\mu g\,l^{-1}$)	1.62 ± 0.07	0.945 ± 0.045
Riboflavin (50 $\mu g\,l^{-1}$)	1.46 ± 0.09	0.904 ± 0.062
Cyanocobalamine (25 $\mu g\,l^{-1}$)	1.51 ± 0.08	0.913 ± 0.067
D-Biotin (200 $\mu g\,l^{-1}$)	1.69 ± 0.08	0.968 ± 0.045
Pyridoxal phosphate (20 $\mu g\,l^{-1}$)	1.38 ± 0.10	0.855 ± 0.065

[a] Bacteria were grown in GMSM at 33.3 °C for 25 h, pH 7.6 with addition of different vitamin sources separately except in control. Data are the mean of triplicates ± S.D.

ting moist. This lyophilized powder was used for detail analysis. The experiments were carried out five times and the values were expressed in means ± standard deviations. Elemental composition of the material is included in Table 4.

Table 3d
Effective supplements on enhanced growth and EPS production by the isolate *Bacillus megaterium* RB-05.[a]

Supplements	Growth (O.D. at 600 nm)	EPS ($g\,l^{-1}$)
Control	0.38 ± 0.11	0.144 ± 0.059
Glucose	1.56 ± 0.09	0.895 ± 0.055
Glucose + L-aspergine	1.45 ± 0.19	0.925 ± 0.051
Glucose + L-aspergine + D-biotin	1.78 ± 0.11	1.121 ± 0.062

[a] Bacteria were grown in GMSM with L-aspergine (0.5% w/v), D-biotin (200 $\mu g\,l^{-1}$) supplementation; control represents mineral salt media without any carbon source at 33.3 °C for 25 h, pH 7.6. Data are the mean of triplicates ± S.D.

Table 4
Components and elemental composition of crude EPS produced by *Bacillus megaterium* RB-05.

Components	Weight (%)
Carbohydrate	87.7 ± 2.5
Protein	8.0 ± 1.8
Uronic acid	1.3 ± 0.5
Others	3.0 ± 0.9
Carbon	43.5 ± 2.8
Hydrogen	7.4 ± 0.6
Nitrogen	1.4 ± 0.3
Oxygen	47.5 ± 2.6
Others	0.2 ± 0.04

3.5. Morphology and physico-chemical features

Both under SEM and TEM the EPS appeared as a cementitious material (Fig. 3). Electron micrograph clearly portrayed association of the EPS molecules with bacterial cells forming EPS based cell cluster, some times in the form of a film. Transmission electron image confirmed the agglomeration of polysaccharides in a chain like conformation. Stronger attractions between the available functional groups within these macromolecules in comparison to the solvent system may be responsible for EPS aggregation (Goh, Haisman, & Singh, 2005). UV–vis spectral analysis of EPS of *B. megaterium* RB-05 showed a strong absorption peak at 220–238 nm range for typical polysaccharide material whereas, another weak absorption peak at 280 nm range, which signifies the presence of a small amount of protein with EPS. Some typical polysaccharide absorption peaks were observed in the FT-IR spectrum of the EPS. Four bands appeared at 3397, 2928, 1658 and 1465 cm^{-1} correspond to the stretching vibrations of –OH, C–H, C=C, and symmetric bending of CH_3 respectively. Absorption peaks in higher frequencies are the most common characteristics of polysaccharides (Silverstein & Webster, 1998; Stuart, 2004). The absorption peak observed at 1286 cm^{-1} is indicative of C–N of amides, which in turn indicates the presence of amino sugars within the polysaccharides. The absorbance frequency in the range of 1658 cm^{-1} also depicts the carbonyl stretching band of amides, a typical characteristic of acetamido groups in N-acetylated sugars. In fact, most of the amino sugars found in microbial EPS are usually N-acetylated (Christensen, 1989). Absorption peak at 861 cm^{-1} is indicative index of α-glycosidic linkage between individual glycosyl residues existed in EPS (Kodali et al., 2009). In addition, a medium-broad C–O stretching was observed around 1062 cm^{-1}, which may be due to ether linkages present within oligomers. X-ray diffractograms exhibited the non-crystalline nature of the material with a single broad peak at around 15–45°, which is very similar to the observation of Xu, Li, Kennedy, Xie, and Huang (2007).

3.6. In vitro free radical scavenging activity

The superoxide radical is a harmful reactive oxygen species as it damages cellular components in biological systems. The ability of the EPS material and standard quercetin to quench superoxide radicals is presented in Fig. 4a. IC_{50} (half maximal inhibition concentration) values of the EPS and standard quercetin were found 24.14 ± 0.94 $\mu g\,ml^{-1}$ (r^2 = 0.9939) and 39.01 ± 1.2 $\mu g\,ml^{-1}$ (r^2 = 0.9652) respectively indicating that the EPS is a superior superoxide radical scavenger than quercetin. Almost 90%

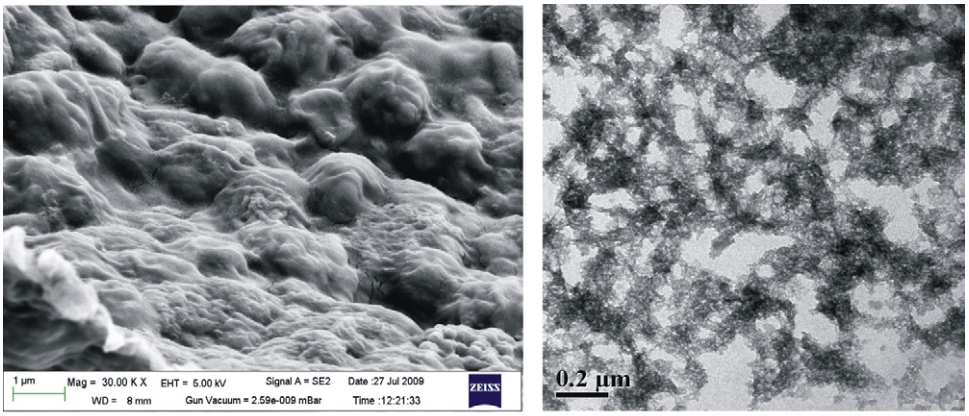

Fig. 3. Different micrographs EPS produced by *B. megaterium* RB-05. Cell mass was embedded within EPS in FeSEM image (a) cementitious EPS in TEM image (b).

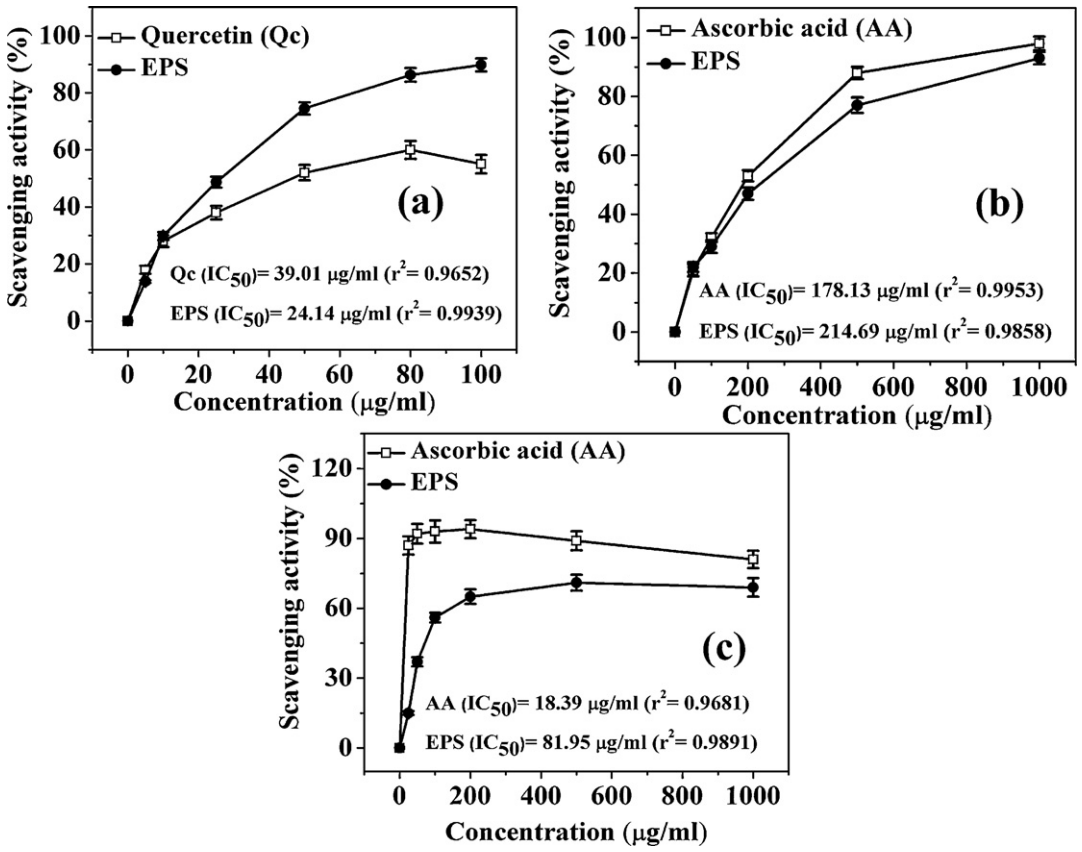

Fig. 4. Free radical scavenging activities and IC_{50} values of the EPS along with standard positive controls. Superoxide radicals (a); hydroxyl radicals (b); and DPPH radicals (c). Data are the mean of six measurements ± S.D.

of the superoxide radicals were engulfed by the EPS material (100 μg ml^{-1}). Free hydroxyl radicals are also very detrimental to the biomolecules of the living cells. The EPS (1000 μg ml^{-1}) and standard ascorbic acid (1000 μg ml^{-1}) showed 93% and 98% scavenging activities respectively for hydroxyl radicals. As evidenced from the IC_{50} values of Fig. 4b, the EPS was found with lower potency of hydroxyl radical scavenging than ascorbic acid, although it is almost equally effective scavenger at higher concentrations. The EPS showed a moderate dose-dependent scavenging activity of DPPH radical scavenging (Fig. 4c) with IC_{50} value of 81.95 ± 2.7 μg ml^{-1} (r^2 = 0.9891), which is inferior to that (18.39 ± 0.7 μg ml^{-1}, r^2 = 0.9681) of positive control ascorbic acid. The EPS may not be as effective as the reference compound with respect to IC_{50} value for DPPH radical scavenging, but showed almost 71% scavenging activity in compared to the 89% of the standard at same concentration (500 μg ml^{-1}). Aforesaid results of *in vitro* free radical study suggests that the EPS material is a potent free radical scavenger and eligible for further *in vivo* studies.

4. Conclusions

B. megaterium RB-05 was found to secrete EPS rapidly in GMSM as maximum production (0.895 g l^{-1}) was achieved within 25 h of incubation. Both process parameters and media conditions for a suitable production system were optimized. Kinetic coefficients suggest for the possible scale up production. According to the kinetic models, EPS production was found to be growth associated as maximum specific growth rate (μ_{max}) and specific EPS production rate were calculated to be (r_p) 0.65 ± 0.01 h^{-1} and 0.215 g g^{-1} cell respectively. Glucose was found as the most effective amongst all the carbon sources used and EPS production was enhance up to 1.12 ± 0.062 g l^{-1} with L-aspergine and D-biotin supplementation. Elemental study and FT-IR spectra confirmed the preliminary composition and functional groups of the EPS. Cementitious nature of this polysaccharide material probably holds the cells together with riverine sediments in such dynamic environment. IC_{50} values of the EPS promise its potency as a free radical scavenger in *in vitro* studies.

References

Calazans, G. M. T., Lopes, C. E., Lima, R. M. O. C., & De Franc, F. P. (1997). Antitumor activities of levans produced by *Zymomonas mobilis* strains. *Biotechnology Letters*, *19*, 19–21.

Chen, H. X., Zhang, M., & Xie, B. J. (2005). Components and antioxidant activity of polysaccharide conjugate from green tea. *Food Chemistry*, *90*, 17–21.

Chen, W., Zhao, Z., Chen, S. F., & Li, Y. Q. (2008). Optimization for the production of exopolysaccharide from *Fomes fomentarius* in submerge culture and its antitumor effect *in vitro*. *Bioresource Technology*, *99*, 3187–3194.

Christensen, B. E. (1989). The role of extracellular polysaccharides in biofilms. *Journal of Biotechnology*, *10*, 181–202.

Cui, F. J., Li, F., Xu, Z. H., Xu, H. Y., Sun, K., & Tao, W. Y. (2006). Optimization of the medium composition for production of mycelial biomass and *exo*-polymer by *Grifola frondosa* GF9801 using response surface methodology. *Bioresource Technology*, *97*, 1209–1216.

Divyashree, M., Rastogi, N., & Shamala, T. (2009). A simple kinetic model for growth and biosynthesis of polyhydroxyalkanoate in *Bacillus flexus*. *New Biotechnology*, *26*, 92–98.

Dubois, M., Gilles, K. A., Hamilton, J., Rebers, P. A., & Smith, F. (1956). Colorimetric method for determination of sugar and relative substances. *Analytical Chemistry*, *28*, 350–366.

Francis, F., Sabu, A., Madhavan, K. N., Sumitra, R., Sanjoy, G., George, S., et al. (2003). Use of response surface methodology for optimizing process parameters for the production of α-amylase by *Aspergillus oryzae*. *Biochemical Engineering Journal*, *15*, 107–115.

García-Garibay, M., & Marshall, V. M. E. (1991). Polymer production by *Lactobacillus delbrueckii* subsp. *Bulgaricus*. *Journal of Applied Bacteriology*, *70*, 325–328.

Garraway, M. O., & Evans, R. C. (1984). Inorganic nutrients. In M. O. Garraway, & R. C. Evans (Eds.), *Fungal nutrition and physiology* (pp. 124–170). New York, USA: Wiley.

Goh, K. K. T., Haisman, D. R., & Singh, H. (2005). Examination of exopolysaccharide produced by *Lactobacillus delbrueckii* subsp. *Bulgaricus* using confocal laser scanning and scanning electron microscopy techniques. *Journal of Food Science*, *70*, 224–229.

Jiao, Y.-C., Chen, Q.-H., Zhou, J.-S., Zhang, H.-F., & Chen, H.-Y. (2008). Improvement of exo-polysaccharides production and modeling kinetics by *Armillaria luteovirens* Sacc. in submerged cultivation. *LWT-Food Science and Technology*, *41*, 1694–1700.

Kalil, S. J., Maugeri, F., & Rodrigues, M. I. (2000). Response surface analysis and simulation as a tool for bioprocess design and optimization. *Process Biochemistry*, *35*, 539–550.

Kishk, Y. F., & Al-Sayed, H. M. (2007). Free-radical scavenging and antioxidative activities of some polysaccharides in emulsions. *LWT-Food Science and Technology*, *40*, 270–277.

Kodali, V. P., Das, S., & Sen, R. K. (2009). An exopolysaccharide from a probiotic: Biosynthesis dynamics, composition and emulsifying activity. *Food Research International*, *42*, 695–699.

Kono, T., & Asai, T. (1969). Kinetics of fermentation processes. *Biotechnology and Bioengineering*, *11*, 293–313.

Kumar, S., Tamura, K., & Nei, M. (2004). An integrated software for Molecular Evolutionary Genetics Analysis and sequence alignment. *Briefings in Bioinformatics*, *5*, 150–163.

Lee, I. Y., Seo, W. T., Kim, G. J., Kim, M. K., Ahn, S. G., Kwon, G. S., et al. (1997). Optimization of fermentation conditions for production of exopolysaccharide by *Bacillus polymyxa*. *Bioprocess Engineering*, *16*, 71–75.

Lin, E. S., & Chen, Y. H. (2007). Factors affecting mycelial biomass and exopolysaccharide production in submerged cultivation of *Antrodia cinnamomea* using complex media. *Bioresource Technology*, *98*, 2511–2517.

Liu, J., Luo, J., Ye, H., Sun, Y., Lu, Z., & Zeng, X. (2009). Production, characterization and antioxidant activities in vitro of exopolysaccharides from endophytic bacterium *Paenibacillus polymyxa* EJS-3. *Carbohydrate Polymers*, *78*, 275–281.

Lowry, O. H., Rosebrough, N. J., Farr, A. L., & Randall, R. J. (1951). Protein measurement with the Folin phenol reagent. *Journal of Biological Chemistry*, *193*, 265–275.

Luedeking, R., & Piret, E. L. (1959). A kinetic study of the lactic acid fermentation: Batch process at controlled pH. *Journal of Biochemical and Microbiological Technology Engineering*, *1*, 393–431.

Monod, J. (1949). The growth of bacterial cultures. *Annual Review of Microbiology*, *3*, 371–394.

Montgomery, D. C. (1997). Response surface methods and other approaches to process optimization. In D. C. Montgomery (Ed.), *Design and analysis of experiments* (pp. 427–510). New York, USA: John Wiley and Sons.

Panda, B., Jain, P., Sharma, L., & Mallick, N. (2006). Optimization of cultural and nutritional conditions for accumulation of poly-β-hydroxybutyrate in *Synechocystis* sp. PCC 6803. *Bioresource Technology*, *97*, 1296–1301.

Pearson, W. R., & Lipman, D. J. (1988). Search for DNA homologies was performed with FASTA program. *Proceedings of National Academy of Sciences*, *85*, 2444–2448.

Roseiro, J. C. (1992). Medium development for xanthan production. *Process Biochemistry*, *27*, 167–175.

Sambrook, J., Fritsch, E. F., & Maniatis, T. (1989). (2nd ed). *Molecular cloning: A laboratory manual* New York, USA: Cold Spring Harbor Laboratory Press.

Sharon, N., & Jeanloz, R. W. (1960). The diaminohexose component of a polysaccharide isolated from *Bacillus subtilis*. *Journal of Biological Chemistry*, *235*, 1–5.

Shih, I. L., Pan, K., & Hsieh, C. (2006). Influence of nutritional components and oxygen supply on the mycelial growth and bioactive metabolites production in submerged culture of *Antrodia cinnamomea*. *Process Biochemistry*, *41*, 1129–1135.

Silverstein, R. M., & Webster, F. X. (1998). Infrared spectroscopy. In R. M. Silverstein, & F. X. Webster (Eds.), *Spectrometric identification of organic compounds* (pp. 71–143). New York, USA: John Wiley & Sons.

Souza, M. C. O., Roberto, I. C., & Milagres, A. M. F. (1999). Solid-state fermentation for xylanase production by *Thermoascus aurantiacus* using response surface methodology. *Applied Microbiology and Biotechnology*, *52*, 768–772.

Stuart, B. H. (2004). Organic molecules. In B. H. Stuart (Ed.), *Infrared spectroscopy: Fundamentals and applications* (pp. 44–70). New Jersey, USA: John Wiley & Sons.

Sutherland, I. W. (2001). Microbial polysaccharides from Gram-negative bacteria. *International Dairy Journal*, *11*, 663–674.

Vanhaverbeke, C., Heyraud, A., & Mazeau, K. (2003). Conformational analysis of the exopolysaccharide from *Burkholderia caribensis* strain MWAP71: Impact of the interaction with soils. *Biopolymers*, *69*, 480–497.

Wang, X., Xu, P., Yuan, Y., Liu, C., Zhang, D., Yang, Z., et al. (2006). Modeling for gellan gum production by *Sphingomonas paucimobilis* ATCC 31461 in a simplified medium. *Applied and Environmental Microbiology*, *72*, 3367–3374.

Xu, X., Li, B., Kennedy, J. F., Xie, B. J., & Huang, M. (2007). Characterization of konjac glucomannan–gellan gum blend films and their suitability for release of nisin incorporated therein. *Carbohydrate Polymers*, *70*, 192–197.

Zheng, Z. M., Hu, Q. L., Jian, H., Feng, X., Guo, N. N., & Yan, S. (2008). Statistical optimization of culture conditions for 1,3-propanediol by *Klebsiella pneumoniae* AC 15 via central composite design. *Bioresource Technology*, *99*, 1052–1056.